Aus der Klinik für Neurochirurgie
der Medizinischen Fakultät Charité – Universitätsmedizin Berlin

DISSERTATION

Support vector machine based aphasia classification of
transcranial magnetic stimulation language mapping in brain
tumor patients

Support-Vector-Machine basierte Aphasie-Klassifikation von
transkraniellem magnetisch stimuliertem Sprach-Mapping bei
Hirntumorpatienten

zur Erlangung des akademischen Grades
Doctor medicinae (Dr. med.)

vorgelegt der Medizinischen Fakultät
Charité – Universitätsmedizin Berlin

von

Ziqian Wang

aus Jilin, China

Datum der Promotion: 26th June 2022

Einleitende Anmerkungen

Einleitende Anmerkungen

Teilergebnisse dieser vorliegenden Arbeit wurden veröffentlicht in:

Wang Z, Dreyer F, Pulvermüller F, Ntemou E, Vajkoczy P, Fekonja LS, Picht T. Support vector machine based aphasia classification of transcranial magnetic stimulation language mapping in brain tumor patients. Neuroimage Clin. 2021;29:102536. doi: 10.1016/j.nicl.2020.102536. Epub 2020 Dec 24. PMID: 33360768; PMCID: PMC7772815[1].

Table of contents

1 Table of contents

Table of contents

List of figures

2   List of figures

3 List of abbreviations

AAL3	Automated anatomical labeling atlas 3rd version
AAT	Aachen aphasia test
ANTs	Advanced normalization tools
BAS	Berlin Aphasia Score
ER	Error rate
FSL	FMRIB software library
IIT	Illinois Institute of Technology
MNI	Montreal neurological institute
PCA	principal component analysis
RFE	recursive feature elimination
ROI	Region of interest
ROC	receiver operating characteristic
RMT	Resting motor threshold
rTMS	Repetitive transcranial magnetic stimulation
SVM	support vector machine
SyN	Symmetric Normalization
VAS	visual analog scale
WHO	World health organization

4 Abstract

4.1 Abstract auf Deutsch

Einleitung: Die navigierte repetitive transkranielle Magnetstimulation (rTMS) ermöglicht die transiente Störung lokaler neuronaler Funktionen auf nicht-invasive Weise. Da Patienten eine signifikante Heterogenität in Bezug auf tumorassoziierte Sprachnetzwerkveränderungen und rTMS-Funktionsmapping-Ergebnisse aufweisen, kann die Verwendung von maschinellem Lernen eine effektive Möglichkeit darstellen, rTMS-Sprachmapping-Muster zuverlässig zu klassifizieren.

Methode: Präoperatives navigiertes rTMS-Sprachmapping wurde bei 90 rechtshändigen Patienten mit linksperisylvischen WHO-Grad II-IV-Gliomen durchgeführt. Zur Beurteilung des Schweregrades der Aphasie wurde der vom Aachener Aphasie-Test (AAT) adaptierte Berlin Aphasia Score (BAS) eingesetzt. Nach der räumlichen Normalisierung aller rTMS-Spots auf den standardisierten Raum des Montreal Neurological Institute (MNI) wurden die Sprachfehlerraten (ER) in jeder der 28 stimulierten kortikalen Areale (ROIs) mit Hilfe der automatisierten anatomischen Parzellierung (AAL3) des Illinois Institute of Technology (IIT) berechnet. Signifikant aphasieassoziierte Regionen wurden mit Hilfe einer Support-Vektor-Maschine (SVM) klassifiziert.

Ergebnisse: Von 90 Patienten in der vorliegenden Studienkohorte lag bei 29 (32,2 %) eine Aphasie vor. Nach Eingabe der demographischen Daten und der ERs jeder ROI in ein SVM-Modell wurde festgestellt, dass die Merkmale, die am signifikantesten zum Gesamtmodell beitrugen, das Alter (w = 2,98) sowie die ERs des linken Gyrus parietalis inferior (w = 2,28), des linken Gyrus supramarginalis (w = 3,64) und der rechten Pars triangularis (w = 1,34) waren. Die Gesamtwerte für Sensitivität, Spezifität und Genauigkeit des Modells betrugen jeweils 86,2 %, 82,0 % bzw. 85,5 %, mit einem AUC-Wert von 89,3 %.

Abstract

Zusammenfassung: Unsere Daten zeigen eine erhöhte Vulnerabilität für rTMS induzierte Sprachfehler in den linken posterioren perisylvischen Arealen, wie dem Gyrus supramarginalis oder dem Gyrus parietalis inferior, was die Sprachrelevanz des klassischen und erweiterten Wernicke-Areals bestätigt. Weiterhin deutet die Beteiligung der rechten inferioren Pars triangularis bei links perisylvischen Gliom-Patienten mit Aphasie auf eine funktionell wichtige Rolle für diese Region hin. Das hier verwendete SVM-Modell wurde nicht durch die Tumorlokalisation beeinflusst, die durch den Vergleich überlappender Regionen mit Atlanten der grauen und weißen Substanz bestimmt wurde. Das SVM-Modell wurde am deutlichsten durch Einschluss des linken supramarginalen Gyrus als Merkmal verbessert. Unsere Daten bestätigen auch, dass das Potential für Neuroplastizität mit zunehmendem Alter abnimmt.

Abstract

4.2   Abstract in English

Background: Neuronavigated repetitive transcranial stimulation (rTMS) permits the transient disruption of local neuronal functions in a non-invasive manner. As patients exhibit significant heterogeneity with respect to tumor-associated language network changes and rTMS functional mapping results, the utilization of machine learning approaches may represent an effective means of classifying rTMS language mapping patterns in a reliable manner.

Method: Presurgical neuronavigated rTMS language mapping was performed in 90 right-handedness patients with left perisylvian WHO grade II-IV gliomas. The Berlin Aphasia Score (BAS) adapted from the Aachen Aphasia Test (AAT) was employed to assess aphasia severity. Following spatial normalization to standardized Montreal Neurological Institute (MNI) space of all rTMS spots, the error rate (ER) of language mapping in each of 28 stimulated cortical regions of interest (ROIs) by the use of automated anatomical labeling parcellation (AAL3) and Illinois Institute of Technology (IIT). Significant aphasia-associated regions were classified using a support vector machine (SVM).

Results: Of 90 patients in the present study cohort, symptoms of aphasia were present in 29 (32.2%). After feeding the demographic data and ERs of each ROI into an SVM model, the features found to contribute most significantly to the overall model included age (w = 2.98), as well as the ERs of the left inferior parietal gyrus (w = 2.28), left supramarginal gyrus (w = 3.64), and right pars triangularis (w = 1.34). Overall model sensitivity, specificity, and accuracy values were 86.2%, 82.0%, and 85.5%, respectively, with an AUC value of 89.3%.

Conclusions: Our data show enhanced vulnerability in the left posterior perisylvian areas, such as the supramarginal gyrus or the inferior parietal gyrus, confirming the language relevance of the classic and extended Wernicke's area. Further, the susceptibility of the right inferior pars triangularis for rTMS in left perisylvian glioma patients with aphasia suggests a functionally important role for this region in aphasia. The SVM model used herein was unaffected by

Abstract

glioma location, which was determined by comparing overlapping regions with atlases of grey and white matter. Our SVM model was improved most significantly by the use of the left supramarginal gyrus as a feature. Our data also confirm that the potential for neuroplasticity decreases with age.

Introduction

5.   Main text

5.1   Introduction

In general, tumor situated in the perisylvian region of the left hemisphere has an inherent risk of causing aphasia. One decade ago, our team introduced rTMS as a tool enabling personalized cortical language mapping in order to guide the surgical treatment of brain tumors[2]. As patients exhibit significant heterogeneity with respect to tumor-associated language network changes and rTMS functional mapping results, the utilization of machine learning approaches may represent an effective means of classifying rTMS language mapping patterns in a reliable manner.

5.1.1 History and current models of language network

Over time, awareness of language processing has gradually increased. In 1865, the French physician, Pierre-Paul Broca, discovered that the left inferior frontal cortex played an role of vital importance during the language production based on autopsy results[3]. In the same way, it was revealed by Carl Wernicke in 1874, a German neurologist, that the left inferior temporal region served an essential position during the procedure of language comprehension[4]. Wernicke likewise emphasized that Broca's area and Wernicke's area are connected, and aphasia could be caused through damage to language centers, for instance, Wernicke's area and Broca's area, as well as damage to their pathways. In 1885, Ludwig Lichtheim summarized and systematized the work of Broca and Wernicke, leading to the classic "Wernicke-Lichtheim model"[5]. In 1970, the Wernicke-Lichtheim model was revised by Norm Geschwind as the "Wernicke-Geschwind model"[6]. After the millennium, the theory of a "dual stream model", as put forth by Hickok and Poeppel et al., has been extensively embraced[7]. It is assumed that the ventral stream, rooted in the bilateral temporal lobes, supports relevant auditory information processing, making it critical for the appropriate comprehension thereof. The auditory-articulatory information is processed by the dorsal stream and is organized unilaterally in the frontal phonological region of the left hemisphere, as well as at the temporoparietal junction[7, 8]. The dorsal stream yields both proprioceptive and auditory feedback, making it essential to fluent speech production[9]. At present, neurological models of semantic and phonological perception suggest these assemblies to be bilaterally distributed with

differential lateralization within perisylvian and extrasylvian sensorimotor and multimodal regions[10].

However, the impact of tumors on language has considerable individual differences. In certain situations, the tumors located in language network related area did not lead to an extensive damage to language even after the total resection[11-14]. In this set up, one interpretation was tumor-induced neural reorganization[15]. Thus, detecting neural reorganization not only assists in performing more radical resections of the tumor, enabling patients to achieve higher benefit/risk ratios but likewise assists in avoiding the postoperative language dysfunction resulted from resection of the reorganized language-related functional areas[11, 16].

5.1.2   r TMS mapping method

In 1985, Barker put forward the first transcranial magnetic stimulation (TMS) designed for the stimulation of human brain. Subsequently, neuronavigated rTMS served a crucial function in cognitive neuroscience study, as well as clinical preoperative planning, because of the features of non-invasiveness and low side effects. rTMS inhibits the electrical bio-signals transmission through the induction of a series of magnetic field pulses. When transcranial magnetic stimulation excites cortical areas (e.g. motor areas), the corresponding target muscles are excited and subsequently contracted, which is capable of being observed through the neurophysiological techniques, for instance, electromyography; when rTMS briefly impedes cortical areas (e.g. language areas) and causes effects that interfere with task performance, a transient "lesion" pattern, which is similar to that of direct electrical stimulation (DES) is produced. Thus, rTMS shares the highest similarity in principle with the 'gold standard', i.e. DES, and denotes an alternative to DES for non-invasive brain mapping. Comparing with DES, rTMS demonstrated variable correspondence in terms of localizing the cortical areas for language processing[17].

5.1.3 Support vector machine

To evaluate complex language networks with regards to aphasia and rTMS object naming results, one viable approach involves the utilization of machine learning (ML) strategies. In contrast to conventional statistical methods, machine learning has more

Introduction

suitable predictive power and concentrates on classification and regression analysis in rich and complex data, and can equally be utilized to infer data[18]. The most prominent classification methods frequently applied nowadays are: logistic regression, neural networks, decision trees, Bayes classification, K-nearest neighbor classification, support vector machine (SVM). Between the period of 1992 and 1995, the SVM was developed on the basis of the statistical learning theory. The basis of the SVM is the Vapnik-Chervonenkis theory, along with the structural risk minimization principle that pursues the most compromise between model complexity and learning ability according to restricted sample information to acquire the most appropriate generalization ability. SVM is already considered to be a suitable development of conventional classifiers and reveal several distinctive advantages to solve small-sample along with high-dimensional ML problems. Moreover, SVM has been revealed to perform better than traditional methods, for instance, in biogenic selection related to cancer. SVM tends to maximize classification margins and be more robust than more conventional analysis methods (e.g. multivariate logistic regression), particularly when considering the analysis of a large feature space and data imbalance[19].Previous researches had illustrated linear SVM methods based on recursive feature elimination (RFE) have a better ability of selecting biological relevant features than classical correlation methods, for example, as in studies of cancer-related gene selection.[20].

This study was designed to employ a machine learning approach for the retrospective assessment of rTMS language mapping results in order to classify patients with and without aphasia in a rich feature space composed of the rTMS language mapping error rate for particular regions together with patient clinical data and lesional profiles.

Methods & Materials

5.2 Methods & Materials

5.2.1 Participants

In total, 296 patients included in our prospective database with left perisylvian brain tumors that had undergone preoperative rTMS language mapping since 2010 were evaluated for this study. The standardized consensus protocol was used to perform rTMS examination on 218 of these patients[21]. Of these patients, 147 had glioma, and 90 of these patients had complete formal language testing (AAT/BAS) results and other data, including 49 males and 41 females with an average age of 48.86 ± 14.12 years (range: 21–82). Of these patients, 12, 42, and 36 had WHO II°, III°, and IV° tumours, resepectively. For further information regarding this patient population, see Table 1. The Edinburgh handedness inventory was used to establish handedness[22]. Patients were excluded from this study if they exhibited aphasia associated with an error rate > 28% in the object naming task, given that this was previously shown to be an effective reliability threshold (Schwarzer et al., 2018). Also, patients who were left-handed, diagnosed with multicentric gliomas, or experienced more than one generalized seizures per week were excluded from this study.

5.2.2 rTMS

Neuronavigated rTMS language mapping was conducted using rTMS eXimia NBS version 3.2.2, Nexstim NBS 4.3 and the NexSpeech module (Nexstim Oy, Helsinki, Finland). Prior to the rTMS mapping, the patients were shown the black-and-white drawings of common objects 3 times (baseline naming task, n = 150), and misnamed images were discarded after each showing. Following the baseline naming task, the remaining images (M = 85.5, SD = 28.6, Min = 35, Max = 149) were presented to the patients consequently with the rTMS stimulation in random sequence during the rTMS mapping (Fig 1). Individual stimulation intensity corresponded to 100% of the patient's resting motor threshold (RMT) of the first dorsal interosseous muscle of the contralateral hand measured utilizing the 5/10 method on the ipsilateral hemisphere's primary motor cortex[23]. Briefly, RMT denotes the lowest TMS intensity that is able to cause MEPs with an amplitude of at least 50 µV in 5 out of 10 stimuli with the first dorsal interosseous muscle in a relaxed state. The black and white objects left from the baseline naming task were presented on a screen in front of the patient. At the

Methods & Materials

onset, the TMS parameters were set for inter-picture interval of 4.0s, picture presentation time of 1000ms, and stimulation frequency of 5Hz. In case the stimuli had no effect on naming over the first 20-30 rTMS trains, these parameters could be sequentially modified to inter-picture interval 2.5s, picture presentation time 700ms, stimulus frequency 7Hz, and 10Hz to augment the challenges. Each patient underwent rTMS mapping for targeting the cortical language function areas within a week following MRI scanning. For each hemisphere, stimulation was conducted at 50-80 distribution sites, each adressed a minimum of three times, as the condition of the patient will allowed. During mapping, the level of discomfort or pain was assessed using a visual analog scale (VAS). The entire process was recorded and analyzed offline. rTMS spots were classified as being either negative or positive, and rTMS-positive spots indicated that rTMS stimulation elicited any form of error response, meanwhile negative spots indicated no error response. rTMS mapping coordinates of the stimulation points were derived for following spatial normalization.

Fig. 1: Performing the rTMS mapping.

5.2.3 Aphasia grading

Preoperative estimation of aphasia severity was conducted with the use of the BAS. The development and application of the BAS was done through the physicians of the Charité University Hospital and adapted to the Aachen Aphasia Test. The patients were classified into four categories by the BAS test: 0 (61 patients) = no aphasia, 1 = mild aphasia (18 patients), 2 = moderate aphasia (8 patients), 3 = severe aphasia (3 patients). The entire patients having a BAS score of 0 were grouped into the non-aphasic group, others were classified as aphasic patients (n = 29). All patients underwent the BAS assessment on the day of rTMS examination.

5.2.4 Data preprocessing

5.2.4.1 Skull striping

Skull stripping is a preliminary step performed to achieve optimal results for spatial normalization of structural MRI data. This method removes the skull, as well as other non-brain tissues from the T1 MRI. These non-brain tissues might impact the robustness and accuracy of spatial normalization which was the next step of data preprocessing. In order to obtain optimal skull striping results, we compared the state-of-art skull striping toolbox, namely FMRIB software library (FSL) and Advanced Normalization Tools (ANTs). In FSL, we used the parameters and approaches proposed by Popescu et al. which is to remove the neck first and then set f=0.1 and option "B" in the brain extraction tool[24]. We used the IXI template to evaluate brain tissue boundaries (https://figshare.com/articles/dataset/ANTs_ANTsR_Brain_Templates). Precisely, the brain with skull template, brain with cerebellum probability mask template and brain with cerebellum registration mask were utilized during the skull striping. From Figure 2, the visually inspection confirms that ANTs had better performance on skull striping than FSL, having less amount of non-brain tissues. In the red and yellow ellipses, it is demonstrated that the FSL results cut off normal brain tissue, whereas the ANT results did not cut off any more brain tissue after stripping the skull. Thus, we consistently utilized ANTs for skull stripping in all patients.
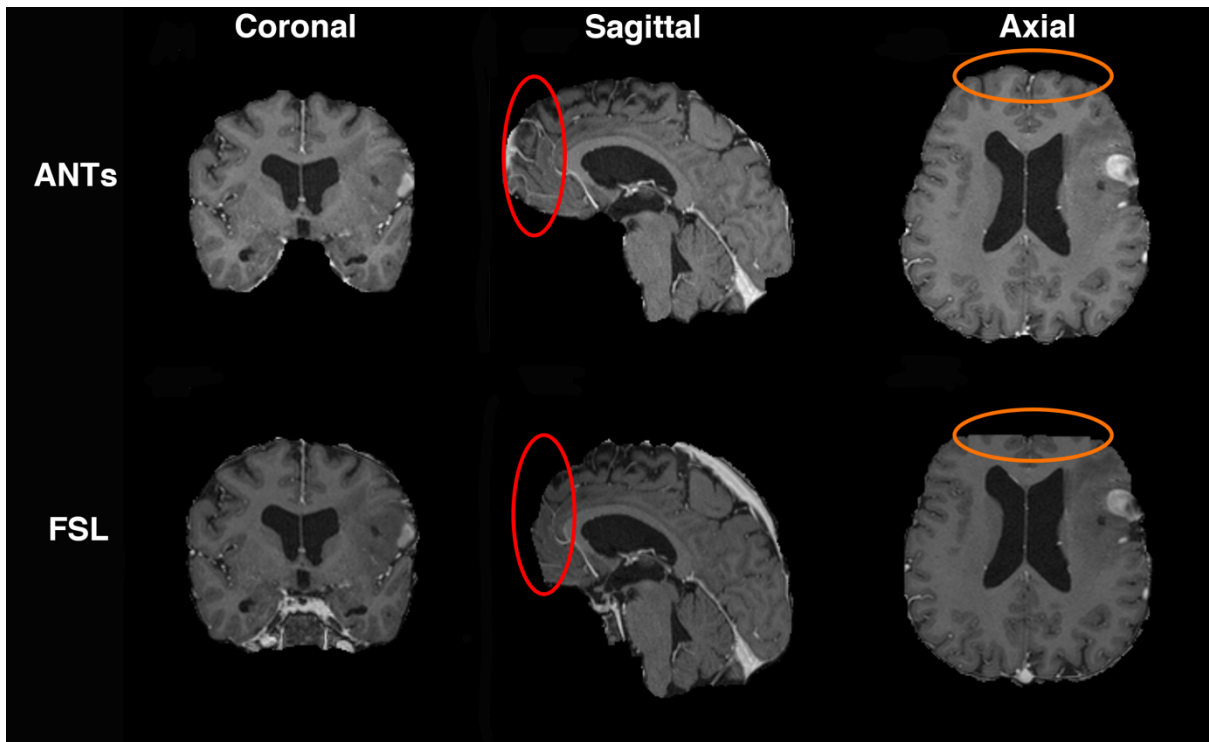
Fig. 2: Comparison of skull striping result between FSL and ANTs. The figure shows the comparison skull striping result of ANTs and FSL on one patient. The first row shows the results for ANTs and the second row shows the results for FSL on the coronal, sagittal and axial view, respectively.

5.2.4.2   Lesion masking

We used a semi-automatic approach to segment the tumor, based on the open source software ITK-SNAP (http://www.itksnap.org). First, we activated the "segmentation 3D" mode. Then, appropriate lower and upper thresholds were manually set to compose the tumor and try to exclude the normal brain tissue. After that, we set seeds inside the structure of interest in order to fill it. The resulting lesions masks were visually inspected and corrected if needed.

Methods & Materials

5.2.4.3   Registration to MNI space

Spatial normalization serves as a method to co-register the various patients' T1 images to a standard space. In our study, we co-registered to montreal neurological institute (MNI) space. The spatial normalization of tumor patients has usually been a challenge since the tumor's inhomogeneous signal intensity in the anatomical image affects the normalization result. The tumor profile of each patient was depicted by the method mentioned in the previous section. The unmasked region of the anatomical image was firstly registered and subsequently utilized the same warping parameters in normalizing the masked area, see Figure 3. All patients' skull striped images were normalized to standard space (MNI space) with ANTs-based Symmetric Normalization (SyN) transformation[25]. The coordinates of the stimulations earlier derived from rTMS mapping were likewise transformed from the individual space to the standard space (i.e., MNI space) through the application of the matrix generated during normalization.
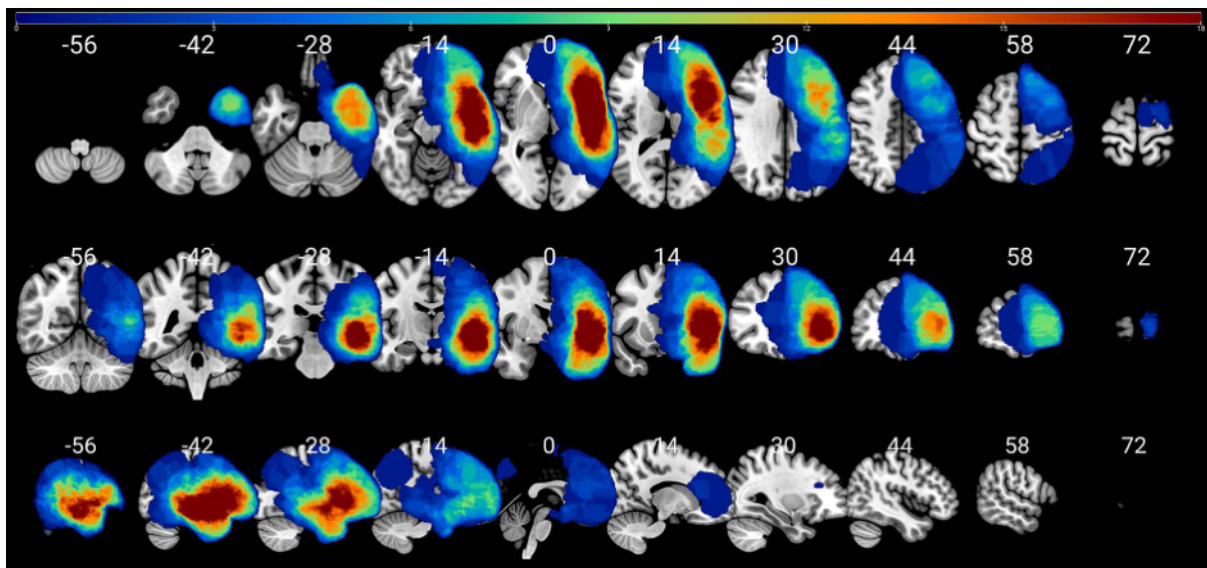

Fig. 3:   Lesion map MNI space lesion maps along with sagittal, coronal, and axial coordinates being shown above corresponding slices. All lesions were perisylvian. Numbers of tumors per voxel are indicated with a colorimetric scale. Own illustration, 2021.

5.2.5 Atlas and error rate

To calculate overlap between tumor masks and atlas regions as a percentage, the MNI template brain was parcellated by applying the automated anatomical labeling atlas, 3rd version (AAL3) and Illinois Institute of Technology (IIT) atlas[26]. For the xjView toolbox (ww.alivelearn.net/xjview), the normalized rTMS spot coordinates were input for obtaining which ROI of the AAL3 atlas each rTMS spot belongs to. After obtaining the entire rTMS spots of the ROI, the error rate (ER) was computed for each ROI per patient, i.e. the amount of error naming TMS stimulations divided by the amount of all rTMS stimulation in this ROI. For example, if a patient's one ROI was stimulated 10 times and 5 times the objects were incorrectly named. The ER was 5 divided by 10, which was 50%. Meanwhile, tumor location can be demonstrated by the proportion of tumor overlap on different ROIs of AAL3 and IIT.

5.2.6 SVM

SVM represents a structural risk minimization principle-based supervised machine learning. SVM denotes a binary classification model whose main focus is to determine the optimal classifying hyperplane that is maximally separates the two groups of samples. When it is not feasible to distinguish the training samples in a linear way, the relaxation factor or penalty coefficients can be introduced to relax the limitations and enable them to be partially tolerant to classification errors. The non-linear problem in the original space tends to likewise be solved through mapping the samples to a higher dimensional space by a non-linear kernel, for example, polynomial kernel, Gaussian kernel and Sigmoid kernel. Provided that in this study our focus is not solely on the classification results but likewise on the weight of the features during the classification, a linear kernel function is adopted. In our dataset, patients were categorized into aphasic or non-aphasic groups on the basis of BAS scores. The TMS ER, age, gender, tumor WHO grade, and principal component analysis (PCA) components of individual IIT and AAL3 lesion percentage for each AAL3 region of the patients were entered into the SVM model as features. As regards to missing data, we discovered that TMS ER was not normally distributed, therefore we utilized median interpolation, denoted as SVM1. To investigate the effect of missing data on the final results, we accordingly applied two more methods, K-NN interpolation (SVM2) and exclusion of 26 patients

Methods & Materials

who failed to undergo rTMS in the right hemisphere (SVM3).

In this study, RFE method was utilized for feature selection in eliminating redundant and irrelevant features. During the construction of a linear classifier, it utilizes the magnitude of the effect of each feature on the objective function as a coefficient for ranking. Assuming it is feasible to express linear classification surface as $f(x) = w \cdot x + b$, then the parameter to construct the ranked list of features is the weight vector size, meaning, the impact size on the objective function. The larger the weight, the higher the influence on the decision function n, as well as the greater the amount of discriminative information it has. The algorithm removes one feature at a time with the least absolute value of weight, and subsequently retrains the classifier to perform the above iterative steps once more, therefore iterating until the feature ranking list is constructed. To enhance the generalization ability of the SVM model, we utilized nested cross-validation for training[27]. Nested cross-validation uses an internal cross-validation loop (5-fold crossover) in adjusting parameters (e.g., penalty parameter C) and select the best model. Parameters C were assessed from 2^{-10} to 2^{10} in steps of 0.1. Data were separated into 5 subsets. One of them was assigned to the test set, while the rest were assigned to the training set. Next, optimization parameter C was estimated from the highest average classification procedure. To assess the selected model through the internal loop, an external cross-validation validation loop (10-fold crossover) was utilized. The data were classified proportionally into 10 subsets, i.e., each subset retained the same proportion of each class as the whole data. Regarding these subsets, one was assigned to the test set, while the others were assigned to the training set, and the results acquired from the test set were utilized for assessing parameters, including the model's accuracy sensitivity and specificity. To reduce the variance, we included a model aggregation method known as bagging and cross-validation to the model. In each iteration, 1000 training sets, as well as corresponding models are generated through random resampling, which determine the final classification outcomes in a voting manner[28] (Figure 4). For machine learning coding, I learned the MATLAB language and the basics of SVM, and we applied MATLAB R2014b (MathWorks, Natick, MA, US), with modifications and additions based on the script of LIBSVM[29]. We assess the performance of the SVM model as regards sensitivity, specificity, overall accuracy, and area under the receive

operating curve (AUC).

It was possible that tumor location could serve as a predictive factor of aphasia status, however, the previous SVM model could conceal this information. Thus, binary logistic regression was applied for analyzing the correlation between the percentage of impairment of a particular ROI through and aphasia status. The percentage of impairment for a specific ROI, defined as the area covered between the ROI and the tumor divided by the total ROI area. Prior to conducting the other analyses, we computed the variance inflation coefficient between each ROI. Since adjacent ROIs tended to show correlations between their tumor overlap, which was due to the anatomical relationship between ROIs, such correlations were capable of causing problems of multicollinearity. To prevent this problem, we set that if the variance inflation coefficient was higher than 5, we would perform principal component analysis on the data to avoid multicollinearity. The results of PCA were entered as predictors in the binary logistic regression model. To assess whether the prediction of aphasia status was impacted through tumor location, we subsequently performed a mediation analysis. Mediated analysis added mediating variables to a simple model with only dependent and independent variables and proposed that independent variables influence (unobservable) mediating variables, which in turn influence dependent variables. Thus, the role of the mediating variable was to specify the character of the relationship between the independent and dependent variables. The Matlab script which was used for the SVM model was published on Zenodo (https://doi.org/10.5281/zenodo.3727663). The SVM pipeline was illustrated by Figure 4.
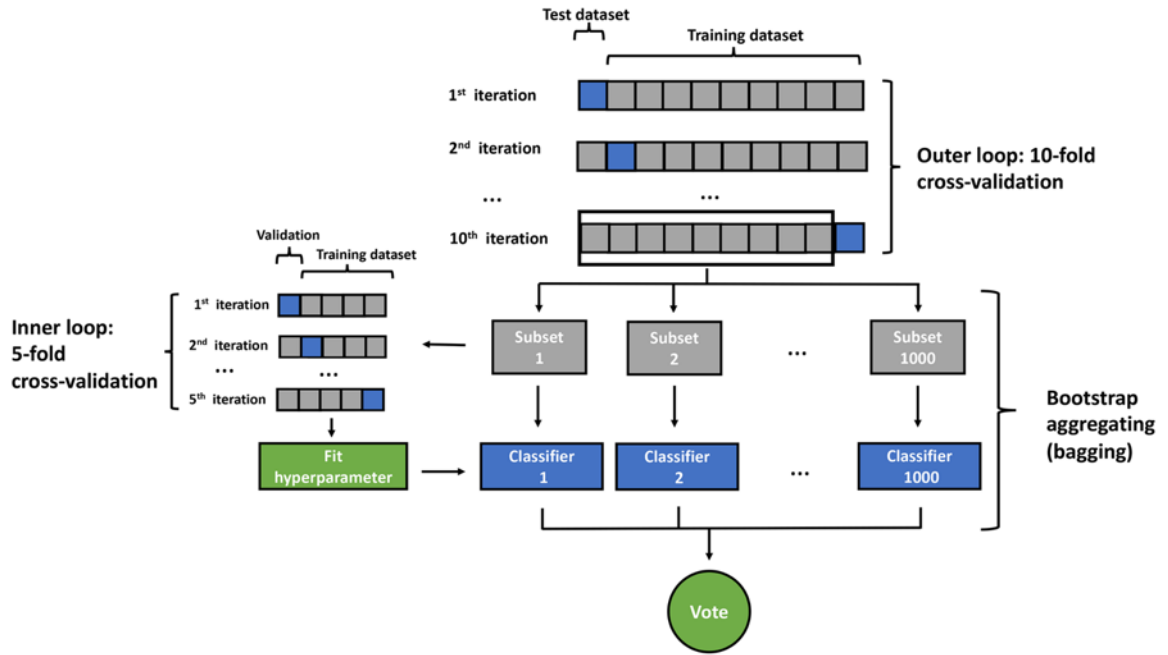
Methods & Materials

Fig. 4: SVM analysis pipeline. Nested cross-validation and bootstrap aggregating (bagging). Own illustration, 2021.

5.2.7 Statistical analysis

Statistical analysis was conducted by MATLAB R2014b (MathWorks, Natick, MA, US) and SPSS 22 (IBM SPSS, Armonk, New York, US). Categorical variables were analyzed using Chi-Squared test. It was feasible to divide continuous variables into normal and non-normal distributions. As regards normal distribution, the two tailed Student's t-test analysis is applied, while in the case of non-normal distribution, the Mann-Whitney U tests analysis is utilized. The statistical significance was set at P-value less than .05. For ER comparisons, the p-values were adjusted using the Holm-Bonferroni method. Spearman's rank correlation was applied for detecting the correlation between BAS and AAT T-scores since the BAS was categorical data.

Results

5.3   Results

Out of the 90 patients recruited, 29 (32.2%) demonstrated preoperative aphasia, i.e., a BAS score higher than 0. No significant difference exists between gender or tumor size and aphasia (χ^2=1.207 [1, 90], p=.272; t[88]=0.023, p=.982). Patients with aphasia were elder (56.69 ± 13.64) compare to those without aphasia (45.13 ± 12.84), p = .0003 (t[52] = 3.83). Out of all the patients in this study, twenty-six patients (19 non-aphasic, 7 aphasic) were mapped only in their left hemisphere due to fatigue or decreased attention. The number of missing ER data points in the AAL3 ROI for the entire patients was 28.8%.

5.3.1 Presurgical rTMS mapping

Mean VAS scores during rTMS mapping were 3.9 ± 2.9 in the left hemisphere and 3.7 ± 2.8 in the right hemisphere. The ER of the entire brain mapping was significantly higher in the aphasic group (Mdn = 7.49) than in the non-aphasic group (Mdn = 3.48) (P < .0001, Z = 4.60, η2 = 0.24). Additionally, ERs were significantly higher in the left hemisphere of aphasic patients compare to those in non-aphasic patients (aphasic: M = 8.87, SD = 4.66, non-aphasic: M = 4.55, SD =3.06, p = .000001), and the difference in ERs in the right hemisphere was insignificant (aphasic: M = 6.71, SD = 4.93, non-aphasic: M = 5.01, SD = 3.67, p = .232). There was no clear pattern in the overall rTMS positive or negative spot distribution, with no prejudice toward specific cortical regions (Figure 5). Whereas, the evaluation of the ERs distribution as regards to rTMS in aphasic and non-aphasic patients depicted specific cortical patterns (Figure 6). The number of stimuli per AAL3 ROI/patient was M = 14.9, SD = 16.2. ERs from the AAL3 ROI that were stimulated above 6 times (> = 25% of stimuli per AAL3 ROI/patient) had been included. A threshold of > = 25% led to a total inclusion of 28 AAL3 ROIs per patient.

Results
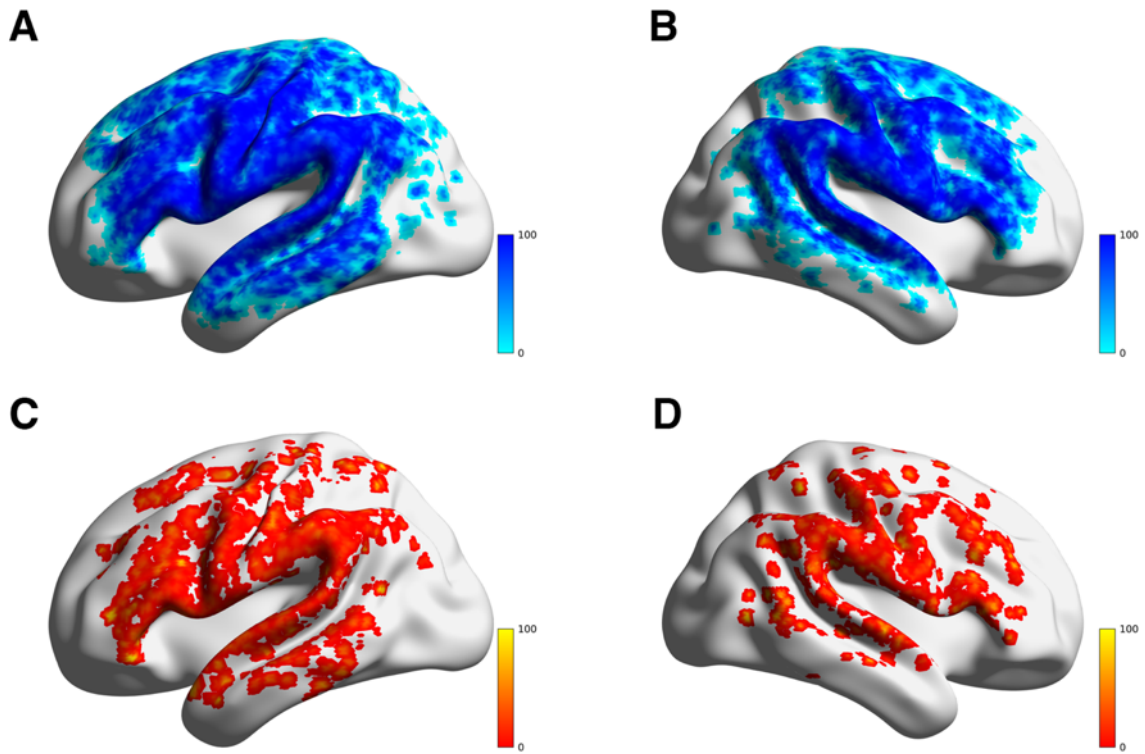
Fig. 5: Voxel-wise rTMS stimulation percentages in the MNI space for all patients. Negative spots on the top left (A) and right (B). Positive spots on the bottom left (C) and right (D). Numbers and color bars correspond to the number of negative or positive stimulations per voxel. Own illustration, 2021.

Fig. 6: Overall ER distributions associated with AAL3 parcellation in groups of patients with (right) and without (left) aphasia. The median ER per region is indicated by color bars. Own illustration, 2021.

Results

5.3.2 SVM results

We fed the entire 28 ERs of ROIs, age, gender, glioma location PCA components, and glioma WHO grade as features to SVM-RFE models for classifying aphasic status. The final classification accuracy values of the three missing data processing methods for SVM1-3 were 85.53%, 82.4% and 77.6%, respectively. The sensitivity value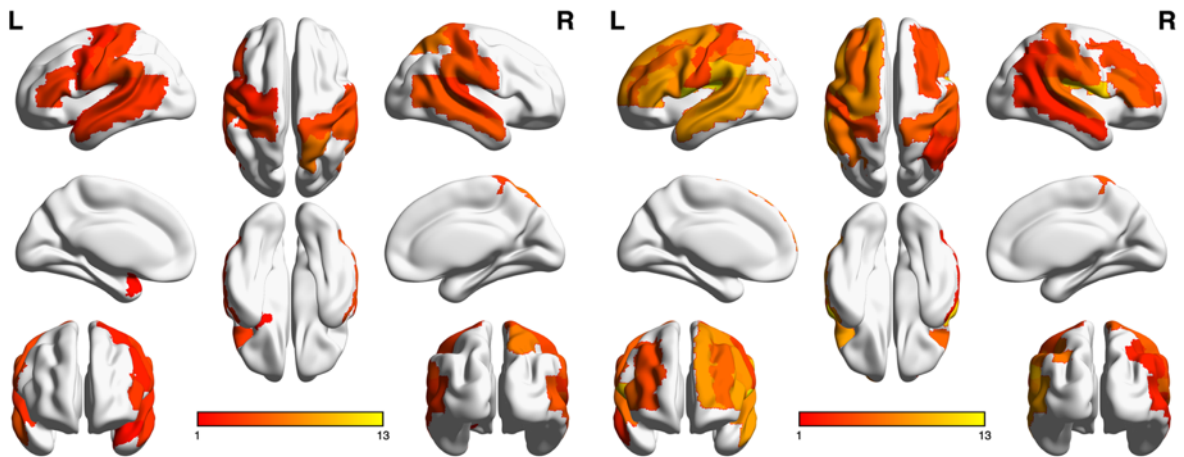s for these three methods were 86.2%, 90.0% and 59.1%, respectively, with corresponding specificity values of 82.0%, 78.7% and 85.7%, and with AUC values of 89.3%, 86.7% and 74.8%. Four features were chosen as the most essential features based on their weights (Fig 7). These four features were age (W = 2.98), ER of the right pars triangularis (W = 1.34), the left supramarginal gyrus (W = 3.64) and the left inferior parietal gyrus (excluding the angular and superior gyrus, W = 2.28). The ERs of these three ROI's differed significantly between groups with and without aphasia after FDR correction (Figure 8).

We computed the overlap between the tumor and the white matter template IIT and the gray matter template AAL3. Since we solely included patients whose tumors were situated in the left perisylvian areas, only 69 ROIs (AAL3, 170 ROIs; IIT, 24 ROIs) overlapped with the tumors out of a total of 194 ROIs (AAL3, 48 ROIs; IIT, 21 ROIs). The variance inflation coefficients of the 69 ROIs ranged from 6 to 10, demonstrating that the overlap ratio between the ROIs there was strong multicollinearity. Subsequently PCA was applied for reducing the data dimensionality, also a total of 10 PCA components were extracted with a Kaiser-Meyer-Olkin value = 0.717. It is revealed from the logistic regression of these 10 PCA components for aphasia status classification that significant results are obtained from component 6 and PCA component 9 (p = .023, Exp(B) = 1.85; p = .005, Exp(B) = 2.36). Based on mediation regression equation showed on Fig 9, we found no complete mediation and only component 6 as a partial mediation between ER of left supramarginal gyrus and aphasia status. Therefore, mediation analysis revealed that tumor location failed to provide explanation for the full predictive value of TMS-induced ER for aphasic status.
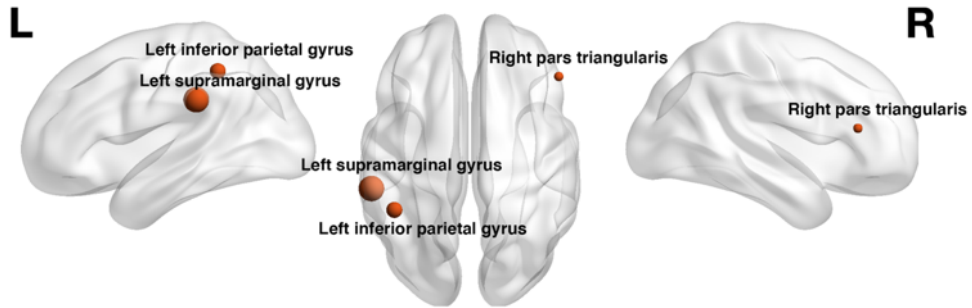
Results

Fig. 7:   Visualization of spherical ROIs-based SVM (SVM1) weights. Own illustration, 2021.
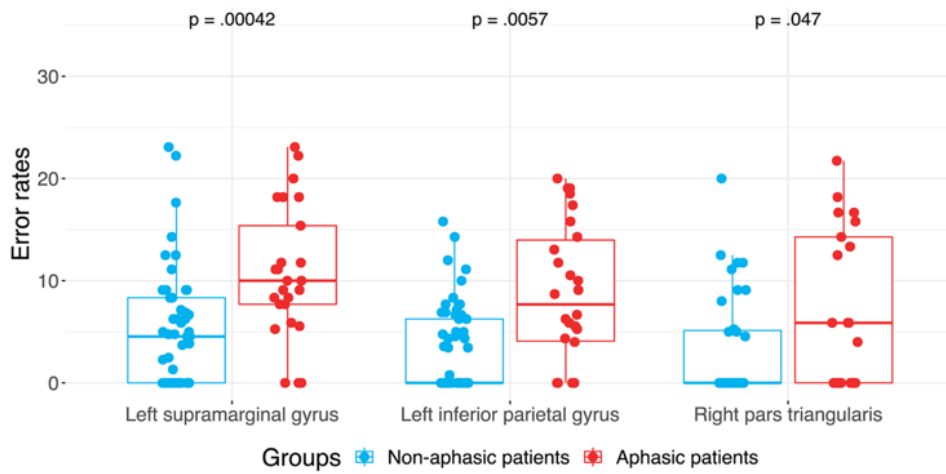

Fig. 8:   Comparison of ERs in patients with and without aphasia based upon SVM (SVM1)-derived AAL3 ROIs. Own illustration, 2021.
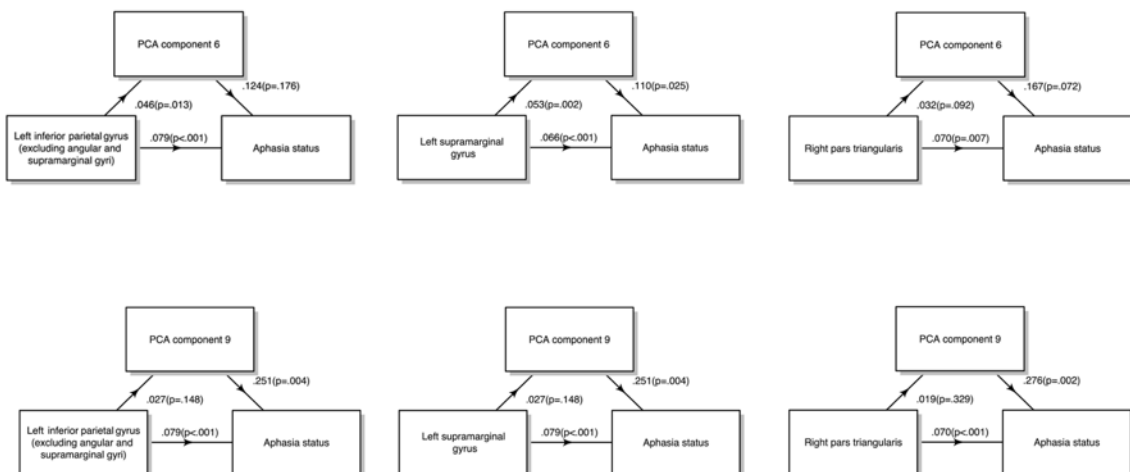

Fig. 9:   Mediation regression results. Own illustration, 2021.

Results

5.4   Discussion

In this study, rTMS language mapping was performed in 90 patients with gliomas in their left perisylvian area, and subsequently SVM were applied in classifying the aphasia status of them (aphasic or non-aphasic). As regarding the SVM results, though the tumors were located in the left hemisphere in all patients, the ER of right pars triangularis had a high classification weight. There could be a correlation between this finding and the current neuroplasticity model, with activation predominantly in bilateral frontal brain regions, which is in line with the post-stroke aphasia studies[30]. As regards the rTMS spots distribution, after we separately mapped positive and negative stimulations to the standard brain, it was discovered that the pattern of the overall negative rTMS spots as well as the pattern of overall negative rTMS spots are not observably different. Furthermore, the rTMS-based analysis revealed that the distribution of rTMS-positive cortical areas around the bilateral hemispheres suggests a bilateral clustering of language functions around the perisylvian areas. This observation corroborates with other research indicating a crucial role for language function in the right triangularis, as well as in the left precentral, central, and parietal regions. The wide rTMS-positive response distribution aligns with language being configured in a large-scale distributed network.

The SVM results revealed that the right pars triangularis, left supramarginal gyrus, left inferior parietal gyrus, and age contributed more to the classification model compared to the rTMS induced object naming. ERs in the right pars triangularis were essential to distinguish patients' aphasic status. The possible reason for this is a functional shift in language ability from the left to the right hemisphere as a compensation mechanism based on the initial impact of left hemisphere brain tumors on the language network. Nevertheless, this may be because of behavioral changes resulting from differences in the prenatal function of specific brain regions or differences in the potential in compensating for loss of function due to reorganization of function. In the study by Hartwigsen and Saur et al., early resolution of acute stroke-induced network disruption and network failure was discovered to be revealed in the left pars triangularis, and chronic spontaneous and treatment-induced reorganization was shown in the right pars triangularis[30]. Inhibition of the right pars triangularis may be related with enhanced object naming performance in TMS-induced post-stroke

Results

aphasia patients. This finding has been replicated multiple times, though other studies have reported large inter-patient differences in the effects of inhibitory rTMS on the right pars triangularis in acute stroke patients[31]. Nevertheless, in the case of patients having brain tumors in left hemisphere, an evidence exists that shifting of function to the right hemisphere is connected with more suitable outcomes following surgery. The hypothesis of enhanced functional reserve in patients having a higher bilateral distribution of language function is supported by these results [32, 33]. The present results remain contentious as regards if the effect of right hemisphere neuroplasticity on the aphasic state has a benefit or is detrimental. The difference in right hemisphere ERs may serve as the proof that neuroplasticity compensates for the (otherwise more severe) language impairment after tumor-induced lesions. On the other hand, at least theoretically, right hemisphere neuroplasticity may likewise reflect the mechanism of dysfunction resulting in (increased) aphasia symptoms in the patients explored in this analysis.

The anterior-inferior part of the parietal lobe consists of the angular gyrus and the supramarginal gyrus. They are situated in the junctional area of auditory, somatosensory areas, along with the visual joint cortex, interconnecting the joint cortex of the three regions. Written or typed words initiate activation of the visual cortex, which then sends the information to the angular and supramarginal gyri, where the visual words are recognized. This information is then associated with auditory word forms in Wernicke's area. The supramarginal gyrus belongs to the region of Geschwind territory. Previous stroke studies have shown that this region is anatomically connected to the arcuate fasciculus and is functionally related to the repetition deficit[34]. Interestingly, the atrophy of the direct arcuate fasciculus (from left inferior frontal gyrus to the superior and middle temporal gyrus) doesn't affect the capability of speech repetition. Whereas, the atrophy of supramarginal gyrus or the indirect arcuate fasciculus (from surparmarginal to left inferior frontal gyrus or the superior and middle temporal gyrus) result in speech repetition deficit. Admittedly, the exact region of speech repetition function remains anatomically controversial, with some suggesting a more posterior position, relative to the superior marginal gyrus, in the angular gyrus or even the superior temporal gyrus[35, 36]. However,

Discussion

there is still consensus that the region of speech repetition function is at the temporoparietal junction. And our results obtained through the SVM model corroborate with other present studies.

Our results confirmed the importance of the inferior parietal cortex for language-related processing, as already been shown in the Danilo et al.'s study [37]. At the same time, this result was the further point of convergence to the latest dual-stream model which was proposed by Gregory Hickok and David Poeppel[7]. Briefly, this dual-stream model assumes that the dorsal stream is in charge of articulation and ventral stream is involved in language recognition. In addition, Jiao et al. provided evidence for functional reorganization of recruitment of the Broca's right hemisphere homologous area after resection of inferior parietal cerebral arteriovenous malformations[38]. This evidence is consistent with our findings on the functional reorganization of right pars triangularis.

Age contributes a high weight in the disfluency classification of our SVM model, which might be due to neuroplasticity of patients decreasing with age. This observation confirms previous studies, in which tumor grade and age, but not tumor location, were associated with aphasia incidence when predicting language dysfunction[39]. The notion of a general tumor induced network disconnection - and no mandatory association with specific lesion locations being relevant for aphasia - is supported by this finding[40].

Conclusion

5.5   Conclusion

In summary, our results were based upon the use of an SVM model to classify 90 left perisylvian glioma patients via machine learning and cortical parceling. It was shown that there were clear differences in rTMS-induced error patterns when comparing individuals with and without aphasia. Specifically, we found that aphasic patients exhibited an increase of ERs in the right hemisphere, particularly in the right pars triangularis, together with an expansion of ERs in the overall right perisylvian distribution. These results suggest that the right frontal lobe may be closely involved in the context of functional reorganization associated with aphasia. Although reliably mapping language networks remains challenging for individual patients with brain tumors, these data highlight the promise of machine learning as a means of detecting distinct areas related to functional reorganization in brain tumor patients in the language network. This study is to our best knowledge the first to have conducted a machine learning based classification of rTMS language mapping data for patients with brain tumors.

Bibliography

6 Bibliography

[1]   Wang Z, Dreyer F, Pulvermüller F, Ntemou E, Vajkoczy P, Fekonja LS, Picht T. Support vector machine based aphasia classification of transcranial magnetic stimulation language mapping in brain tumor patients. *Neuroimage Clin*. 2020;29:102536.

[2]   Picht T, Krieg SM, Sollmann N, Rösler J, Niraula B, Neuvonen T, Savolainen P, Lioumis P, Mäkelä JP, Deletis V, Meyer B, Vajkoczy P, Ringel F. A comparison of language mapping by preoperative navigated transcranial magnetic stimulation and direct cortical stimulation during awake surgery. *Neurosurgery*. 2013;72:808-19.

[3]   Dronkers NF, Plaisant O, Iba-Zizen MT, Cabanis EA. Paul Broca's historic cases: high resolution MR imaging of the brains of Leborgne and Lelong. *Brain*. 2007;130:1432-41.

[4]   DeWitt I, Rauschecker JP. Wernicke's area revisited: parallel streams and word processing. *Brain Lang*. 2013;127:181-91.

[5]   Fridriksson J, den Ouden DB, Hillis AE, Hickok G, Rorden C, Basilakos A, Yourganov G, Bonilha L. Anatomy of aphasia revisited. *Brain*. 2018;141:848-62.

[6]   Geschwind N. The organization of language and the brain. *Science*. 1970;170:940-4.

[7]   Hickok G, Poeppel D. The cortical organization of speech processing. *Nat Rev Neurosci*. 2007;8:393-402.

[8]   Ries SK, Piai V, Perry D, Griffin S, Jordan K, Henry R, Knight RT, Berger MS. Roles of ventral versus dorsal pathways in language production: An awake language mapping study. *Brain Lang*. 2019;191:17-27.

[9]   Murakami T, Kell CA, Restle J, Ugawa Y, Ziemann U. Left dorsal speech stream components and their contribution to phonological processing. *J Neurosci*. 2015;35:1411-22.

[10]   Pulvermüller F. Neurobiological Mechanisms for Semantic Feature Extraction and Conceptual Flexibility. *Top Cogn Sci*. 2018;10:590-620.

[11]   Raffa G, Quattropani MC, Scibilia A, Conti A, Angileri FF, Esposito F, Sindorio C, Cardali SM, Germanò A, Tomasello F. Surgery of language-eloquent tumors in patients not eligible for awake surgery: the impact of a protocol based on navigated

Bibliography

transcranial magnetic stimulation on presurgical planning and language outcome, with evidence of tumor-induced intra-hemispheric plasticity. *Clin Neurol Neurosurg.* 2018;168:127-39.

[12]	Duffau H. The error of Broca: From the traditional localizationist concept to a connectomal anatomy of human brain. *J Chem Neuroanat.* 2018;89:73-81.

[13]	Fekonja L, Wang Z, Bährend I, Rosenstock T, Rösler J, Wallmeroth L, Vajkoczy P, Picht T. Manual for clinical language tractography. *Acta Neurochir (Wien).* 2019;161:1125-37.

[14]	Friederici AD, Gierhan SM. The language network. *Curr Opin Neurobiol.* 2013;23:250-4.

[15]	Ghinda CD, Duffau H. Network Plasticity and Intraoperative Mapping for Personalized Multimodal Management of Diffuse Low-Grade Gliomas. *Front Surg.* 2017;4:3.

[16]	Rösler J, Niraula B, Strack V, Zdunczyk A, Schilt S, Savolainen P, Lioumis P, Mäkelä J, Vajkoczy P, Frey D, Picht T. Language mapping in healthy volunteers and brain tumor patients with a novel navigated TMS system: evidence of tumor-induced plasticity. *Clin Neurophysiol.* 2014;125:526-36.

[17]	Picht T, Krieg SM, Sollmann N, Rösler J, Niraula B, Neuvonen T, Savolainen P, Lioumis P, Mäkelä JP, Deletis V, Meyer B, Vajkoczy P, Ringel F. A Comparison of Language Mapping by Preoperative Navigated Transcranial Magnetic Stimulation and Direct Cortical Stimulation During Awake Surgery. *Neurosurgery.* 2013;72:808-19.

[18]	Bzdok D, Altman N, Krzywinski M. Statistics versus machine learning. *Nat Methods.* 2018;15:233-4.

[19]	Musa AB. Comparative study on classification performance between support vector machine and logistic regression. *International Journal of Machine Learning and Cybernetics.* 2013;4:13-24.

[20]	Guyon I, Weston J, Barnhill S, Vapnik V. Gene Selection for Cancer Classification using Support Vector Machines. *Machine Learning.* 2002;46:389-422.

[21]	Krieg SM, Lioumis P, Mäkelä JP, Wilenius J, Karhu J, Hannula H, Savolainen P, Lucas CW, Seidel K, Laakso A, Islam M, Vaalto S, Lehtinen H, Vitikainen AM, Tarapore PE, Picht T. Protocol for motor and language mapping by navigated TMS

in patients and healthy volunteers; workshop report. *Acta Neurochir (Wien)*. 2017;159:1187-95.

[22]   Oldfield RC. The assessment and analysis of handedness: the Edinburgh inventory. *Neuropsychologia*. 1971;9:97-113.

[23]   Rossini PM, Burke D, Chen R, Cohen LG, Daskalakis Z, Di Iorio R, Di Lazzaro V, Ferreri F, Fitzgerald PB, George MS, Hallett M, Lefaucheur JP, Langguth B, Matsumoto H, Miniussi C, Nitsche MA, Pascual-Leone A, Paulus W, Rossi S, Rothwell JC, Siebner HR, Ugawa Y, Walsh V, Ziemann U. Non-invasive electrical and magnetic stimulation of the brain, spinal cord, roots and peripheral nerves: Basic principles and procedures for routine clinical and research application. An updated report from an I.F.C.N. Committee. *Clin Neurophysiol*. 2015;126:1071-107.

[24]   Popescu V, Battaglini M, Hoogstrate WS, Verfaillie SC, Sluimer IC, van Schijndel RA, van Dijk BW, Cover KS, Knol DL, Jenkinson M, Barkhof F, de Stefano N, Vrenken H. Optimizing parameter choice for FSL-Brain Extraction Tool (BET) on 3D T1 images in multiple sclerosis. *Neuroimage*. 2012;61:1484-94.

[25]   Avants BB, Epstein CL, Grossman M, Gee JC. Symmetric diffeomorphic image registration with cross-correlation: evaluating automated labeling of elderly and neurodegenerative brain. *Med Image Anal*. 2008;12:26-41.

[26]   Rolls ET, Huang CC, Lin CP, Feng J, Joliot M. Automated anatomical labelling atlas 3. *Neuroimage*. 2020;206:116189.

[27]   Varoquaux G, Raamana PR, Engemann DA, Hoyos-Idrobo A, Schwartz Y, Thirion B. Assessing and tuning brain decoders: Cross-validation, caveats, and guidelines. *Neuroimage*. 2017;145:166-79.

[28]   Poldrack RA, Huckins G, Varoquaux G. Establishment of Best Practices for Evidence for Prediction: A Review. *JAMA Psychiatry*. 2020;77:534-40.

[29]   Chang C-C, Lin C-J. LIBSVM: A library for support vector machines. *ACM Trans Intell Syst Technol*. 2011;2:Article 27.

[30]   Hartwigsen G, Saur D. Neuroimaging of stroke recovery from aphasia - Insights into plasticity of the human language network. *Neuroimage*. 2019;190:14-31.

[31]   Naeser MA, Martin PI, Theoret H, Kobayashi M, Fregni F, Nicholas M, Tormos JM, Steven MS, Baker EH, Pascual-Leone A. TMS suppression of right pars

triangularis, but not pars opercularis, improves naming in aphasia. *Brain Lang*. 2011;119:206-13.

[32]   Ille S, Kulchytska N, Sollmann N, Wittig R, Beurskens E, Butenschoen VM, Ringel F, Vajkoczy P, Meyer B, Picht T, Krieg SM. Hemispheric language dominance measured by repetitive navigated transcranial magnetic stimulation and postoperative course of language function in brain tumor patients. *Neuropsychologia*. 2016;91:50-60.

[33]   Harvey DY, Mass JA, Shah-Basak PP, Wurzman R, Faseyitan O, Sacchetti DL, DeLoretta L, Hamilton RH. Continuous theta burst stimulation over right pars triangularis facilitates naming abilities in chronic post-stroke aphasia by enhancing phonological access. *Brain Lang*. 2019;192:25-34.

[34]   Forkel SJ, Rogalski E, Drossinos Sancho N, D'Anna L, Luque Laguna P, Sridhar J, Dell'Acqua F, Weintraub S, Thompson C, Mesulam MM, Catani M. Anatomical evidence of an indirect pathway for word repetition. *Neurology*. 2020;94:e594-e606.

[35]   Mesulam MM, Rader BM, Sridhar J, Nelson MJ, Hyun J, Rademaker A, Geula C, Bigio EH, Thompson CK, Gefen TD, Weintraub S, Rogalski EJ. Word comprehension in temporal cortex and Wernicke area: A PPA perspective. *Neurology*. 2019;92:e224-e33.

[36]   Rogalski E, Cobia D, Harrison TM, Wieneke C, Thompson CK, Weintraub S, Mesulam MM. Anatomy of language impairments in primary progressive aphasia. *J Neurosci*. 2011;31:3344-50.

[37]   Bzdok D, Hartwigsen G, Reid A, Laird AR, Fox PT, Eickhoff SB. Left inferior parietal lobe engagement in social cognition and language. *Neurosci Biobehav Rev*. 2016;68:319-34.

[38]   Jiao Y, Lin F, Wu J, Li H, Fu W, Huo R, Cao Y, Wang S, Zhao J. Plasticity in language cortex and white matter tracts after resection of dominant inferior parietal lobule arteriovenous malformations: a combined fMRI and DTI study. *Journal of Neurosurgery JNS*. 2021;134:953.

[39]   Lu T, Pan Y, Kao SY, Li C, Kohane I, Chan J, Yankner BA. Gene regulation and DNA damage in the ageing human brain. *Nature*. 2004;429:883-91.

Bibliography

[40]   Recht LD, McCarthy K, O'Donnell BF, Cohen R, Drachman DA. Tumor-associated aphasia in left hemisphere primary brain tumors: the importance of age and tumor grade. *Neurology*. 1989;39:48-50.

7   Statutory Declaration

"I, Ziqian Wang, by personally signing this document in lieu of an oath, hereby affirm that I prepared the submitted dissertation on the topic *Support vector machine based aphasia classification of transcranial magnetic stimulation language mapping in brain tumor patients* and *Support-Vector-Machine basierte Aphasie-Klassifikation von transkraniellem magnetisch stimuliertem Sprach-Mapping bei Hirntumorpatienten*, independently and without the support of third parties, and that I used no other sources and aids than those stated.

All parts which are based on the publications or presentations of other authors, either in letter or in spirit, are specified as such in accordance with the citing guidelines. The sections on methodology (in particular regarding practical work, laboratory regulations, statistical processing) and results (in particular regarding figures, charts and tables) are exclusively my responsibility.

Furthermore, I declare that I have correctly marked all of the data, the analyses, and the conclusions generated from data obtained in collaboration with other persons, and that I have correctly marked my own contribution and the contributions of other persons (cf. declaration of contribution). I have correctly marked all texts or parts of texts that were generated in collaboration with other persons.

My contributions to any publications to this dissertation correspond to those stated in the below joint declaration made together with the supervisor. All publications created within the scope of the dissertation

Statutory Declaration

comply with the guidelines of the ICMJE (International Committee of Medical Journal Editors; www.icmje.org) on authorship. In addition, I declare that I shall comply with the regulations of Charité – Universitätsmedizin Berlin on ensuring good scientific practice.

I declare that I have not yet submitted this dissertation in identical or similar form to another Faculty.

The significance of this statutory declaration and the consequences of a false statutory declaration under criminal law (Sections 156, 161 of the German Criminal Code) are known to me."

Date   Signature

8 Declaration of your own contribution to the publications

Ziqian Wang contributed the following to the below listed publications:

1. *Wang Z, Dreyer F, Pulvermüller F, Ntemou E, Vajkoczy P, Fekonja LS, Picht T. Support vector machine based aphasia classification of transcranial magnetic stimulation language mapping in brain tumor patients. Neuroimage Clin. 2021*

This study was designed by Thomas Picht, Lucius Fekonja and Ziqian Wang. Ziqian Wang collected the data, including demographic data and image data, and converted the DICOM files to NIFTI file format. To be able to batch process data, Ziqian learned how to use shell scripting and code of FSL （MRIB software library）. With the help of Lucius Fekonja, Ziqian learned how to use ANTs (Advanced Normalization Tools) to process MRI data and registered the coordinates of T1 MRI data and TMS stimulation to MNI standard space. Ziqian Wang drew the lesion masks of most patients with ITK-snap (http://www.itksnap.org). Additionally, Ziqian Wang wrote the MATLAB code for the SVM model. Ziqian Wang analyzed the data with R software (Vienna, Austria) and MATLAB. Ziqian Wang built all the tables and figures according to the comments from the coauthors. All the coauthors took part in the writing of the original draft and made critical revision of the manuscript.

_____
Signature, date and stamp of first supervising university professor / lecturer

_____
Signature of doctoral candidate

9 Auszug aus der Journal Summary List

Journal Data Filtered By: **Selected JCR Year: 2019** Selected Editions: SCIE,SSCI
Selected Categories: **"NEUROIMAGING"** Selected Category Scheme: WoS
Gesamtanzahl: 14 Journale

Rank	Full Journal Title	Total Cites	Journal Impact Factor	Eigenfactor Score
1	NEUROIMAGE	102,632	5.902	0.125360
2	Journal of NeuroInterventional Surgery	5,583	4.460	0.015900
3	HUMAN BRAIN MAPPING	23,094	4.421	0.042760
4	NeuroImage-Clinical	7,868	4.350	0.027050
5	Brain Imaging and Behavior	2,979	3.391	0.008440
6	AMERICAN JOURNAL OF NEURORADIOLOGY	23,135	3.381	0.027120
7	NEUROIMAGING CLINICS OF NORTH AMERICA	1,191	2.632	0.001640
8	JOURNAL OF NEURORADIOLOGY	1,103	2.423	0.001810
9	JOURNAL OF NEUROIMAGING	2,219	2.321	0.004170
10	NEURORADIOLOGY	5,713	2.238	0.006020
11	PSYCHIATRY RESEARCH-NEUROIMAGING	5,414	2.063	0.007190
12	CLINICAL EEG AND NEUROSCIENCE	1,075	1.765	0.001690
13	STEREOTACTIC AND FUNCTIONAL NEUROSURGERY	1,724	1.635	0.002060
14	KLINISCHE NEUROPHYSIOLOGIE	54	0.111	0.000010

1

Selected JCR Year: 2019; Selected Categories: "NEUROIMAGING"

10   Publication

Wang, Z., Dreyer, F., Pulvermüller, F., Ntemou, E., Vajkoczy, P., Fekonja, L. S., & Picht, T. (2021). Support vector machine based aphasia classification of transcranial magnetic stimulation language mapping in brain tumor patients. NeuroImage. Clinical, 29, 102536. https://doi.org/10.1016/j.nicl.2020.102536

Publication

Wang Z, Dreyer F, Pulvermüller F, Ntemou E, Vajkoczy P, Fekonja LS, Picht T. Support vector machine based aphasia classification of transcranial magnetic stimulation language mapping in brain tumor patients. Neuroimage Clin. 2020 Dec 24;29:102536. doi: 10.1016/j.nicl.2020.102536. Epub ahead of print. PMID: 33360768; PMCID: PMC7772815.

Publication

Wang, Z., Dreyer, F., Pulvermüller, F., Ntemou, E., Vajkoczy, P., Fekonja, L. S., & Picht, T. (2021). Support vector machine based aphasia classification of transcranial magnetic stimulation language mapping in brain tumor patients. NeuroImage. Clinical, 29, 102536. https://doi.org/10.1016/j.nicl.2020.102536

Publication

Wang, Z., Dreyer, F., Pulvermüller, F., Ntemou, E., Vajkoczy, P., Fekonja, L. S., & Picht, T. (2021). Support vector machine based aphasia classification of transcranial magnetic stimulation language mapping in brain tumor patients. NeuroImage. Clinical, 29, 102536. https://doi.org/10.1016/j.nicl.2020.102536

Publication

Wang, Z., Dreyer, F., Pulvermüller, F., Ntemou, E., Vajkoczy, P., Fekonja, L. S., & Picht, T. (2021). Support vector machine based aphasia classification of transcranial magnetic stimulation language mapping in brain tumor patients. NeuroImage. Clinical, 29, 102536. https://doi.org/10.1016/j.nicl.2020.102536

Publication

Wang, Z., Dreyer, F., Pulvermüller, F., Ntemou, E., Vajkoczy, P., Fekonja, L. S., & Picht, T. (2021). Support vector machine based aphasia classification of transcranial magnetic stimulation language mapping in brain tumor patients. NeuroImage. Clinical, 29, 102536. https://doi.org/10.1016/j.nicl.2020.102536

Publication

Wang, Z., Dreyer, F., Pulvermüller, F., Ntemou, E., Vajkoczy, P., Fekonja, L. S., & Picht, T. (2021). Support vector machine based aphasia classification of transcranial magnetic stimulation language mapping in brain tumor patients. NeuroImage. Clinical, 29, 102536. https://doi.org/10.1016/j.nicl.2020.102536

Publication

Wang, Z., Dreyer, F., Pulvermüller, F., Ntemou, E., Vajkoczy, P., Fekonja, L. S., & Picht, T. (2021). Support vector machine based aphasia classification of transcranial magnetic stimulation language mapping in brain tumor patients. NeuroImage. Clinical, 29, 102536. https://doi.org/10.1016/j.nicl.2020.102536

Publication

Wang, Z., Dreyer, F., Pulvermüller, F., Ntemou, E., Vajkoczy, P., Fekonja, L. S., & Picht, T. (2021). Support vector machine based aphasia classification of transcranial magnetic stimulation language mapping in brain tumor patients. NeuroImage. Clinical, 29, 102536. https://doi.org/10.1016/j.nicl.2020.102536

Publication

Wang, Z., Dreyer, F., Pulvermüller, F., Ntemou, E., Vajkoczy, P., Fekonja, L. S., & Picht, T. (2021). Support vector machine based aphasia classification of transcranial magnetic stimulation language mapping in brain tumor patients. NeuroImage. Clinical, 29, 102536. https://doi.org/10.1016/j.nicl.2020.102536

Publication

Wang, Z., Dreyer, F., Pulvermüller, F., Ntemou, E., Vajkoczy, P., Fekonja, L. S., & Picht, T. (2021). Support vector machine based aphasia classification of transcranial magnetic stimulation language mapping in brain tumor patients. NeuroImage. Clinical, 29, 102536. https://doi.org/10.1016/j.nicl.2020.102536

11   Curriculum Vitae

My curriculum vitae does not appear in the electronic version of my paper for reasons of data protection.

Curriculum Vitae

12   Complete list of publications

1. Fekonja L, **Wang Z**, Bährend I, Rosenstock T, Rösler J, Wallmeroth L, Vajkoczy P, Picht T. **Manual for clinical language tractography.** Acta Neurochir (Wien). 2019 Jun;161(6):1125-1137. doi: 10.1007/s00701-019-03899-0. Epub 2019 Apr 19. PMID: 31004240; PMCID: PMC6525736.

2. **Wang Z**, Dreyer F, Pulvermüller F, Ntemou E, Vajkoczy P, Fekonja LS, Picht T. **Support vector machine based aphasia classification of transcranial magnetic stimulation language mapping in brain tumor patients.** Neuroimage Clin. 2020 Dec 24;29:102536. doi: 10.1016/j.nicl.2020.102536. Epub ahead of print. PMID: 33360768; PMCID: PMC7772815.

3. Fekonja LS, **Wang Z**, Aydogan DB, Roine T, Engelhardt M, Dreyer FR, Vajkoczy P, Picht T. **Detecting Corticospinal Tract Impairment in Tumor Patients With Fiber Density and Tensor-Based Metrics.** Front Oncol. 2021 Jan 27;10:622358. doi: 10.3389/fonc.2020.622358. PMID: 33585250; PMCID: PMC7873606.

13   Acknowledge

At this moment, I would like to thank all the people who have supported me. Your compliments have given me the motivation to continue my work and your criticisms have made me realize the shortcomings in myself.

I would especially like to thank my two supervisors, the first supervisor Mr. PD Dr.med. Thomas Picht and second supervisor Dr.rer.med Lucius Samo Fekonja. They have been generous and meticulous in helping me, not only in academic research but also in daily life. They have led me into the field of neuroscience and have shown me the way. At the same time, they also helped me to settle into the lab community and the scientific work. Besides, thanks for PH.D. Felix Dreyer. He always can find the novel and genius method to analyze and interpret the data.

In addition, thank my friends as well as my colleagues in *Image Guidance Labs* for their great support and assistance in the preparation of my thesis, which has also been a great inspiration to me.

Finally, I would like to thank my family. Their selfless support and assistance over the years, mentally and physically, is what made me determined to pursue my scientific research career.